PCCP

Accepted Manuscript




ROYAL SOCIETY OF CHEMISTRY

www.rsc.org/pccp

# Aqueous $Fe_2S_2$ cluster: structure, magnetic coupling, and hydration behaviour from Hubbard $U$ density functional theory

Umberto Terranova and Nora H. de Leeuw,

Department of Chemistry,

University College London, London, WC1H 0AJ U.K.;

**Abstract**

We present a DFT+U investigation of the all-ferrous $Fe_2S_2$ cluster in aqueous solution. We determine the value of $U$ by tuning the geometry of the cluster in the gas-phase to that obtained by the highly accurate CCSD(T) method. When the optimised value of $U$ is employed for the aqueous $Fe_2S_2$ cluster ($Fe_2S_2$(aq)), the resulting geometry agrees well with the X-ray diffraction structure, while the magnetic coupling is in line with the estimate from Mössbauer data. Molecular dynamics trajectories predict $Fe_2S_2$(aq) to be stable in water, regardless of the introduction of $U$. However, significant differences arise in the geometry, hydration, and exchange constant of the solvated clusters.

## 1 Introduction

Aqueous iron-sulfur clusters (FeS(aq)), with water molecules molecularly coordinated to the ferrous iron atoms, are of considerable interest to Origins of Life

theories, which suggest that the oxidative formation of pyrite ($FeS_2$), i.e.,

$$FeS(aq) + H_2S = FeS_2 + H_2, \quad (1)$$

could have provided the energy source for the reduction of $CO_2$ into simple prebiotic organic molecules [1].

Electrochemical and mass spectroscopy data have shown that small FeS(aq) are formed rapidly in aqueous solution, where they coexist in equilibrium with the first condensed mackinawite phase (FeS) [2, 3]. However, there is no general consensus on the size and stoichiometry of FeS(aq) [4], and even their stabilities in water have been questioned [5]. Among the variety of complexes suggested, the rhombic $Fe_2S_2$ is particularly interesting, as it is very similar to the basic structural unit of mackinawite [3]. Remarkably, the $Fe_2S_2$ unit constitutes also the active centre of various metalloproteins [6], and it has has been the subject of a number of both experimental [7–9] and theoretical [10–15] investigations (see Ref. [16] for a review on this and other analogues of protein active sites). Unlike in marine systems, however, the all-ferrous state is not common in biology [17–19], as the anionic cysteinate ligands prevent the formation of a cluster with additional negative charge, and favour the Fe(II)/Fe(III) or Fe(III)/Fe(III) combination [20].

Due to strong correlation effects, transition metal (TM) compounds represent a challenge for density functional theory (DFT) [21]. Its uncorrected use translates into contracted geometries and absolute values of magnetic couplings which are too large [22, 23]. In principle, post Hartree-Fock methods are then required to obtain the correct description of the ground state wavefunction [14]. For example, when dealing with closed shell or open shell high-spin (HS) states, the coupled cluster CCSD(T) method can provide excellent structures and is considered the gold standard of quantum chemistry [24]. However, post Hartree-Fock methods limit to a few atoms the size of the affordable system, and it is not surprising that DFT calculations are still the preferential tool to

simulate the behaviour of small TM clusters in solution [25, 26].

Within DFT, one possibility of improving the description of TM compounds is offered by the DFT+U approach [27]. Here, the strongly correlated electrons are treated with the addition of a Hubbard correction, while the others are described by the standard DFT functional. Results depend sensitively on the value of $U$, which can be chosen by fitting relevant properties to experiments or high-level quantum chemistry methods. Alternatively, a linear response approach to calculate in an internally consistent way all the interaction parameters has been developed [28]. Recently, our group and others have applied the DFT+U method to study the electronic and magnetic structures of iron-sulfur minerals such as greigite ($Fe_3S_4$) [29, 30], cubic FeS [31], and pyrite [32, 33]. In addition to applications to bulk systems and surfaces, the DFT+U scheme has also been applied to the $Fe_2$ dimer [34, 35], and to the ferric $[Fe_2S_2(SH)_4]^{2-}$ complex in vacuo [36], where it has been shown to reproduce various properties, including spin splittings, geometries, and harmonic frequencies.

Here, we use DFT+U to carry out an investigation of $Fe_2S_2$ in aqueous solution. First, we determine the strength of the parameter $U$ by tuning its value to reproduce the geometry of the cluster obtained at the CCSD(T) level. Then, we proceed to study the aqueous $Fe_2S_2$ cluster ($Fe_2S_2$(aq)). We show that the Hubbard correction strongly affects its magnetic coupling and structure, as well as the binding energy of water. Finally, we perform molecular dynamics (MD) of $Fe_2S_2$(aq) in water, to determine the effect of adding the $U$ correction in the trajectories. We find that important changes arise in the structure of $Fe_2S_2$(aq), as well as in the number of water molecules that are hydrogen-bonded to the cluster.

# 2 Methods

## 2.1 The broken symmetry approach

As estabilished by Mössbauer data, the biological $Fe_2S_2$ unit is expected to be in the low-spin (LS) state, with the two ferrous iron atoms in the HS configuration ($S_1 = S_2 = 2$), and antiferromagnetically coupled [37]. Thus, in principle, the correct description of the ground state wavefunction would require the use of unaffordable multireference methods [14].

More conveniently, in our DFT scheme, we start the MD trajectories in the broken symmetry (BS) state, i.e. the state where the spins on the two Fe(II) are antiparallel, while the z-component of total spin takes the lowest zero value. Even though the BS differs from the real LS density (the BS spin density is not zero everywhere in space), our choice is partly justified by the fact that, in the $Fe_2S_2(H_2O)_8$ cluster, both DFT and DFT+U predict the BS state to be lower in energy than the HS state (see section 3.2), i.e. the state where the two Fe(II) are ferromagnetically coupled. The BS approach (see Ref. [38] for a complete review), has already been employed to describe the geometric and electronic structure of the $Fe_2S_2$ clusters in proteins [39].

The magnetic coupling between the two HS iron atoms can be described by the Heisenberg Hamiltonian:

$$\hat{H} = -2J\hat{S}_1\hat{S}_2 = -J\big[\hat{S}^2 - \hat{S}_1^2 - \hat{S}_2^2\big], \tag{2}$$

where $\hat{S}_1$ and $\hat{S}_2$ are the spin operators on the two sites, $\hat{S}^2 = (\hat{S}_1 + \hat{S}_2)^2$, and $J$ is the exchange coupling constant. From Eq. 2, it follows that the energies $E_{\mathrm{BS}}$ and $E_{\mathrm{HS}}$, of respectively BS and HS, are given by:

$$E_{\mathrm{BS,HS}} = -J\big[\langle\hat{S}^2\rangle_{\mathrm{BS,HS}} - S_1(S_1+1) - S_2(S_2+1)\big]. \tag{3}$$

With the assumption of no overlap between the magnetic orbitals, the BS ap-

proach uses Eq. 3 to express $J$ as a function of $E_{\mathrm{BS}}$ and $E_{\mathrm{HS}}$:

$$J = \frac{E_{\mathrm{BS}} - E_{\mathrm{HS}}}{S^2_{max}}, \tag{4}$$

where $S_{max} = S_1 + S_2 = 4$.

## 2.2 Computational details

We have employed both Gaussian09 [40] and VASP 5.3 [41, 42] in the study of the gas-phase $Fe_2S_2$, whereas simulations on $Fe_2S_2$(aq) were performed only with VASP. Unless otherwise stated, Gaussian calculations have been carried out with the cc-pVTZ basis set [43], particularly suitable for post Hartee-Fock methods like CCSD(T). In addition to the common PBE functional [44], based on the generalised gradient approximation (GGA), DFT calculations with Gaussian were also performed with M06L [45]. In VASP, we have adopted a plane wave (PW) cutoff of 400 eV, together with the PBE functional, and the projector augmented wave method (PAW) to model the core-electron interaction [46]. Specifically, we have considered the 4s and 3d electrons of Fe, the 3s and 3p of S, the 2s and 2p of O, and the 1s of H as valence electrons, and treated them explicitly. All of the calculations have been performed at the Γ-point. Since VASP implements periodic boundary conditions, in order to avoid spurious interactions between replica atoms, we have introduced a vacuum of at least 12 Å between adjacent cells containing isolated molecules.

Starting coordinates for MD trajectories were taken from the PBE optimised $Fe_2S_2$ unit in the gas-phase, which was then immersed in a 12.416 × 12.416 × 12.416 box of 64 water molecules pre-equilibrated by classical MD. Four water molecules were removed to avoid overlap with the cluster. The final $Fe_2S_2(H_2O)_{60}$ complex was partially optimised, and the structure equilibrated for 10 ps in the DFT Born-Oppenheimer potential energy surface. At this point, the $U$ correction was introduced and a partial optimisation was again followed by another 10 ps of equilibration. We have taken the coordinates of the two

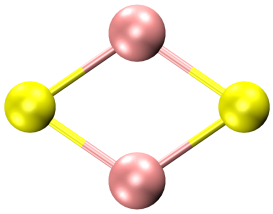

Figure 1: $Fe_2S_2$ cluster (Fe pink, S yellow).

equilibrated systems as the starting configurations for the DFT and DFT+U based MD runs. In all of the trajectories, we have used a time step of 0.5 fs, and a Nosé thermostat [47] at a temperature of 400 K, which is required to reproduce the structural properties of water [48].

# 3 Results and discussion

## 3.1 Gas-phase $Fe_2S_2$

Here we present results for the isolated $Fe_2S_2$ molecule in the HS state (Figure 1), whose single-determinant wavefunction can be described by both DFT and CCSD(T). First, we study the accuracy of various basis sets to predict the HS geometry at the PBE level of DFT. Then, we use the geometry at the CCSD(T) level of theory to calibrate $U$ and find the optimised value for the cluster.

Table 1 compares the geometrical parameters of $Fe_2S_2$ predicted by PBE. Regardless of the basis set, the optimised dihedral $\theta$(Fe–S–Fe–S) angle is always larger than zero, i.e. the molecule is not planar. We note that the LANL2DZ [49] combination of effective core potentials (ECPs) with a double zeta quality valence basis set is not suitable for the description of the cluster. Calculations with the Stuttgart/Dresden ECP bases (SDD [50]) give better geometries than LANL2DZ, as reported in the literature for TM complexes [51], and show that Dirac-Fock relativistic effects are negligible for this study. Given that we aim to calibrate the VASP DFT results with the Gaussian CCSD(T), it is reassuring

| Basis set | $d$(Fe–Fe) | $d$(Fe–S) | $\theta$(Fe–S–Fe–S) |
|---|---|---|---|
| LANL2DZ[a] | 2.30 | 2.31 | 26.0 |
| SDD[ac] | 2.27 | 2.28 | 23.9 |
| SDD[ad] | 2.26 | 2.27 | 23.5 |
| 6-311G+(d)[a] | 2.24 | 2.22 | 24.2 |
| cc-pVDZ[a] | 2.24 | 2.22 | 23.2 |
| cc-pVTZ[a] | 2.23 | 2.21 | 23.2 |
| PW[b] | 2.21 | 2.20 | 23.7 |

Table 1: Bond distances (Å) and dihedrals (degrees) of $Fe_2S_2$ in the HS state calculated with the PBE functional for different basis sets. (a) Gaussian entry; (b) VASP entry; (c) Hartree-Fock ECP; (d) Dirac-Fock relativistic ECP.

that the geometries given by PW and cc-pVTZ (already converged at the cc-pVDZ level, and very similar to 6-311G+(d)), agree well between both codes. The residual difference, not relevant to our purposes, may be attributed to the pseudopotential approximation in VASP.

Table 2 compares the selected properties of $Fe_2S_2$ obtained by different DFT functionals with other level of theories. PBE and M06L predict poor structures which deviate considerably from CCSD(T) and MRCI+Q [14]. This confirms the difficulty of DFT to describe accurately TM compounds even with M06L, which is especially recommended for systems involving TM bonding [45]. It is interesting that not only local functionals, but also the hybrid B3LYP is not able to reproduce the CCSD(T) geometry [15]. Significant improvements are obtained by adding increasing values of $U$ to PBE, whose effect is to increase both $d$(Fe–Fe) and $d$(Fe–S), while gradually reducing the dihedral $\theta$(Fe–S–Fe–S) angle to reproduce the correct planar geometry.

At the HS geometry, local functionals predict the exchange coupling to be positive, i.e. of the wrong sign compared to B3LYP [15] and MRCI+Q calculations [14]. Introducing the Hubbard term in the Hamiltonian reverses this anomaly, and negative values of $J$ are recovered. From this analysis, it is evident that the DFT+U approach improves significantly the description of $Fe_2S_2$. In particular, a value of $U = 5$ eV gives geometrical and magnetic properties which accurately characterise the unit.

| Theory | $d$(Fe–Fe) | $d$(Fe–S) | $\theta$(Fe–S–Fe–S) | $J$ |
|---|---|---|---|---|
| M06L[a] | 2.23 | 2.21 | 20.4 | +204 |
| PBE[b] | 2.21 | 2.20 | 23.7 | +178 |
| $U = 1$[b] | 2.22 | 2.21 | 20.9 | +103 |
| $U = 3$[b] | 2.35 | 2.24 | 14.3 | −95 |
| $U = 5$[b] | 2.56 | 2.27 | 0.0 | −111 |
| CCSD(T)[a] | 2.58 | 2.27 | 0.0 | - |
| B3LYP [15] | 2.41 | 2.25[c] | - | −103 |
| MRCI+Q [14] | 2.62 | 2.30 | - | −70 |

Table 2: Selected geometrical parameters (bonds in Å, dihedrals in degrees), and magnetic coupling ($cm^{-1}$) of $Fe_2S_2$ in the HS state at different levels of theory. (a) Gaussian entry; (b) VASP entry ; (c) mean value of the four bonds.

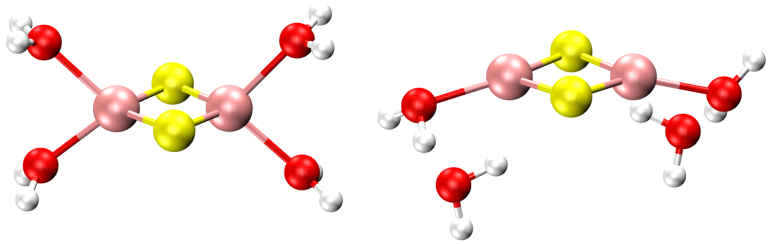

Figure 2: $Fe_2S_2(H_2O)_4$ cluster before (left) and after (right) the optimisation (Fe pink, S yellow, O red, H white).

### 3.2 Aqueous $Fe_2S_2$ cluster

In this section, we investigate the isolated $Fe_2S_2$(aq) proposed in Ref. [52] (Figure 2, left). When applying the DFT+U scheme, we use the value of $U = 5$ eV derived for $Fe_2S_2$ in section 3.1, for both the HS and the BS state. This is justified by the finding that, for the ferric $[Fe_2S_2(SH)_4]^{2-}$ complex, the Hubbard corrections in the BS and HS geometries were found to differ by only 0.05 eV [36].

Regardless of the spin state, both DFT and DFT+U predict the most stable configuration of $Fe_2S_2(H_2O)_4$ to have both irons in a trigonal-planar environment (Figure 2, right). Only one molecule of water is molecularly bound to

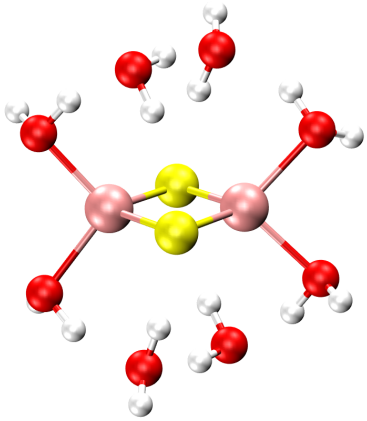

Figure 3: $Fe_2S_2(H_2O)_8$ cluster (Fe pink, S yellow, O red, H white).

each Fe(II) of the cluster, while the remaining two form hydrogen bonds with the S atoms, thereby stabilising their negative charges. We find that the addition of water molecules hydrogen-bonded to the sulfurs spontaneously relaxes the trigonal-planar geometry to the one where the irons are tetrahedrally coordinated. Therefore, we conclude that $Fe_2S_2(H_2O)_4$ is not a good model for $Fe_2S_2$(aq), and move to a $Fe_2S_2(H_2O)_8$ cluster (Figure 3).

Tables 3 and 4 summarise the selected parameters for $Fe_2S_2(H_2O)_8$ in the BS and the higher energy HS state, respectively. They are shown together with the X-ray diffraction geometry and the estimate for $J$ from Mössbauer spectra of an all-ferrous $Fe_2S_2$ cluster bonded to two benzimidazolato ligands, the only all-ferrous $Fe_2S_2$ structure isolated and crystallographically characterised at present [37]. The comparison with the $Fe_2S_2$(aq) must be made with caution, as the benzimidazolato capping ligands are anionic. However, it is interesting that, for both the BS and HS states, the DFT geometrical parameters, especially the Fe–Fe distance, are far from the experimental values. Introducing the Hubbard correction increases all the bond lenghts, and brings the experimental and theoretical geometries to much closer agreement.

In the BS state, water molecules are bound to the $Fe_2S_2(H_2O)_8$ cluster with an energy of $-0.65$ eV. Consistent with the stretching contribution to the

| | BS | | | |
|---|---|---|---|---|
| Theory | $d$(Fe–Fe) | $d$(Fe–S)$^a$ | $J$ | $E_b$ |
| DFT | 2.51 | 2.20 | $-234$ | $-0.65$ |
| DFT+U | 2.76 | 2.33 | $-127$ | $-0.71$ |
| exp[37] | 2.75 | 2.27 | $< -30$ | |

Table 3: Selected geometrical parameters (Å), binding energy per water molecule (eV), and exchange coupling constant ($cm^{-1}$) of $Fe_2S_2(H_2O)_8$ in the BS state. (a) mean value of the four bonds.

| | HS | | | | |
|---|---|---|---|---|---|
| Theory | $d$(Fe–Fe) | $d$(Fe–S)$^a$ | $J$ | $E_b$ | $\Delta E$ (HS − BS) |
| DFT | 2.55 | 2.28 | $-17$ | $-0.62$ | $+0.27$ |
| DFT+U | 2.81 | 2.36 | $-53$ | $-0.72$ | $+0.17$ |

Table 4: Selected geometrical parameters (Å), binding energy per water molecule (eV), and exchange coupling constant ($cm^{-1}$) of $Fe_2S_2(H_2O)_8$ in the HS state. The difference in energy $\Delta E$ with respect to the BS state is also reported (eV). (a) mean value of the four bonds.

structure, a strengthening of the interaction with water results from the DFT+U method, which predicts the binding energy per water molecule to decrease to $-0.71$ eV. We note that the binding energy is little affected by the spin state of the system. Accordingly, during MD, we do not expect the hydration of the cluster to change significantly with spin.

Experiments on the tetranuclear all-ferrous $Fe_2S_2$ unit, with and without the surrounding protein, have only provided upper limits for $J$ [19, 37]. Our DFT estimate is very dependent on the reference geometry, i.e. $-234/-17$ $cm^{-1}$ in the BS and HS state respectively. However, the value of $-127/-53$ $cm^{-1}$ estimated by DFT+U is less affected by the geometry. It is therefore more reliable, and can serve as a valuable reference to experiment.

### 3.3 Aqueous $Fe_2S_2$ in water

As discussed in section 2.1, we have started both the DFT and DFT+U trajectories from the BS electronic configuration, which is the lowest in energy for $Fe_2S_2(H_2O)_8$. Despite not fixing the spin multiplicity, none of the trajectories showed variations from the BS value of zero. We also note that in both runs the

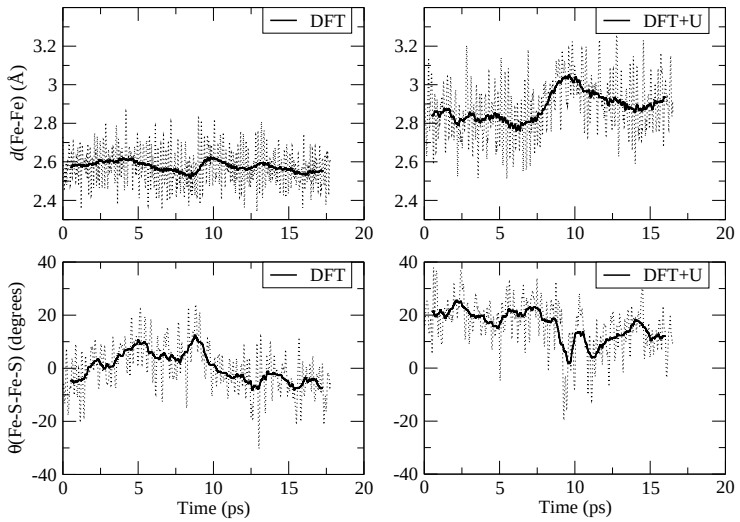


Figure 4: Selected parameters of the $Fe_2S_2$(aq) cluster in water during the MD runs with and without the $U$ correction. Thick lines represent the running averages at 1 ps.

complex does not dissolve at the temperature of 400 K, in agreement with mass spectrometry data predicting $Fe_2S_2$ as the likely monomeric unit of the larger FeS(aq) [3].

Figure 4 illustrates the main geometrical parameters of $Fe_2S_2$(aq) during the MD trajectories in water. The complete solvation allows more water molecules than in $Fe_2S_2(H_2O)_8$ to interact directly with the $Fe_2S_2$ core, and the resulting network of hydrogen bonds causes an increase of the bond lengths in the cluster (Table 5), now larger than those from $Fe_2S_2(H_2O)_8$ and the experimental solvent-free structure (Table 3).

Sulfur K-edge X-ray absorption spectroscopy and DFT calculations have estabilished that hydrogen-bonding of water to the sulfides decreases the Fe–S covalency of iron-sulfur compounds [53, 54]. In turn, this correlates with an increase of their reduction potentials [55–57]. In this work, we are not directly concerned with the electrochemical properties of $Fe_2S_2$(aq). However, the in-

| Theory | $d$(Fe–Fe) | $d$(Fe–S)$^a$ | $\theta$(Fe–S–Fe–S) | Fe-hydr | H-bonds | $J^b$ |
|---|---|---|---|---|---|---|
| DFT | 2.57 | 2.22 | 0.0 | 3/4 | 4.9 | −162 |
| DFT+U | 2.88 | 2.38 | 16.0 | 4/5 | 6.2 | −109 |

Table 5: Summary of the properties predicted by DFT and DFT+U *ab initio* MD: average geometrical parameters (bonds in Å, dihedrals in degrees), possible Fe hydrations, average numbers of hydrogen bonds, magnetic couplings ($cm^{-1}$). (a) mean value of the four bonds; (b) from the respective optimised tetrahedral configurations (Figure 6, middle).

creased Fe–S distances are in line with the weakening of the Fe–S bonds, and previous DFT [58] and nuclear magnetic resonance spectroscopy investigations [59] have reported similar elongations on hydrogen-bonding.

As expected from the investigation of $Fe_2S_2(H_2O)_8$, there are clear differences between the DFT and DFT+U geometries of $Fe_2S_2$(aq), especially reflected in the Fe–Fe distance. At the same time, as indicated by the values of the dihedral angle along the trajectories, while a planar geometry results on average from the DFT run, significant distorsions from it are introduced by the DFT+U. Consistent with the expanded geometry, we note that the effect of the solvent is to reduce the strength of the magnetic coupling with respect to the $Fe_2S_2$ (Table 5). The differences in the geometries are paralleled by the tendency for a larger hydration of the Fe atoms, in line with the lower binding energies of water discussed in section 3.2.

Figure 5 depicts the total number of water molecules molecularly coordinated to the Fe of the cluster. DFT predicts this value to fluctuate between 3 and 4, i.e., in addition to the tetrahedral configuration (Figure 6, middle), a configuration where one of the two Fe is in a trigonal-planar arrangement is also thermodynamically possible (Figure 6, left). A loss of water molecule from the cluster has happened three times during the MD run (including a first time during equilibration). We attempted to relax the structure with a trigonal-planar Fe, but, interestingly, the $Fe_2S_2$(aq) is not stable in this arrangement, and spontaneously relaxes towards the tetrahedral configuration. The dehydration is therefore driven by the gain in entropy resulting from the loss of water. The effect of the Hubbard correction is to raise the total hydration of the Fe

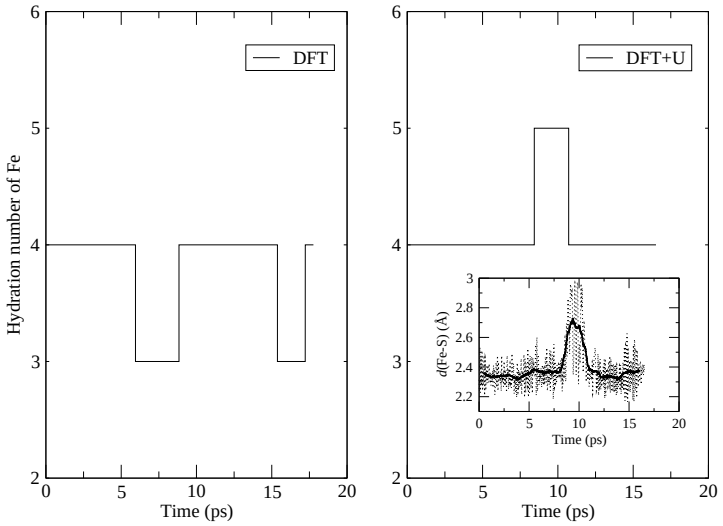


Figure 5: Total hydration number of the Fe ions in the cluster during the MD runs with and without the $U$ correction. Inset: one Fe–S distance during the DFT+U run; the thick line represents the running average at 1 ps.

atoms in the cluster, now varying between 4 and 5. In the second case, one of the two Fe adopts a trigonal bipyramidal geometry (Figure 6, right). When this happens, one of the Fe–S bonds in the cluster stretches considerably (Figure 5, inset). In our run, we have twice observed this attack by a water molecule (a first time during equilibration). In both cases, however, rather than dissociation of the cluster, dehydration occurs after a few picoseconds, re-estabilishing the tetrahedral configuration of both the irons.

At this point, there are two drawbacks to functionals based on GGA which we would like to discuss. It has been found that GGA tends to overstructure liquid water, while hybrid functionals are superior in reproducing its experimental structure and dynamical properties [60]. In addition, a pitfall of GGA is the incorrect description of the long-range dispersive forces, which are essential to soften the water structure [61]. In order to evaluate the effects of hybrid functionals on the structure and solvation of $Fe_2S_2$(aq), we have relaxed the

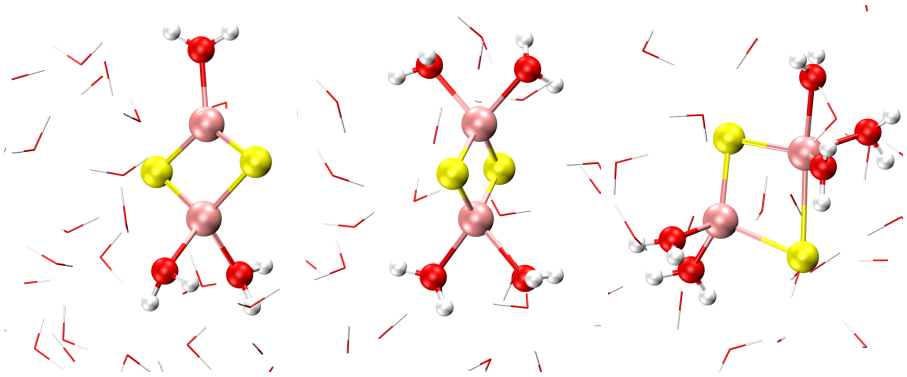

Figure 6: Snapshots of the $Fe_2S_2$(aq) cluster in water. Left: mixed trigonal-tetrahedral Fe (DFT); middle: tetrahedral Fe (DFT and DFT+U); right: mixed tetrahedral-trigonal bipyramidal (DFT+U). Water molecules molecularly bound to the cluster have been emphasised (Fe pink, S yellow, O red, H white).

two DFT+U configurations (Figure 6, middle and right) with the hybrid PBE0 functional [62]. The same structures were also optimised with the addition to DFT+U of the interatomic pair potentials proposed by Grimme [63] (DFT+U-D2), with the purpose of assessing the changes due to inclusion of dispersion corrections.

For both structures, PBE0 and DFT+U predict similar geometries (Table 6), in line with what observed in a study on the ferric $[Fe_2S_2(SH)_4]^{2-}$ complex, where the hybrid B3LYP was compared to DFT+U [23]. While a pronounced effect is evident on the relative stabilities of the two geometries, with PBE0 predicting a smaller difference between the two ground state energies, we do not observe any modification in the solvation shells of $Fe_2S_2$(aq). The structural changes arising when DFT+U-D2 is employed are less important, but they are paralleled by a stabilisation of the tetrahedral configuration. We report in Table 6 the results for the tetrahedral configuration of iron atoms (Figure 6, middle), as changes in the geometry of the tetrahedral-trigonal bipyramidal (Figure 6, right) follow the same trend.

Finally, we discuss the impact of $U$ on the number of hydrogen bonds formed between water and the S ions in the cluster. We have used a O–S distance of 3.7 Å, and a O–H–S angle of 40° as a cutoff for the hydrogen bond criterium.

| Theory | $d$(Fe–Fe) | $d$(Fe–S)$^a$ | $\theta$(Fe–S–Fe–S) | $E_{rel}$ |
|---|---|---|---|---|
| DFT+U | 2.86 | 2.38 | 21.3 | +0.34 |
| PBE0 | 2.81 | 2.34 | 21.4 | +0.17 |
| DFT+U-D2 | 2.88 | 2.38 | 22.0 | +0.16 |

Table 6: Structural parameters (bonds in Å, dihedrals in degrees) of $Fe_2S_2$(aq) corresponding to the tetrahedral configuration of iron atoms (Figure 6, middle). $E_{rel}$ is the energy with respect to the tetrahedral-trigonal bipyramidal configuration (Figure 6, right). (a) mean value of the four bonds.

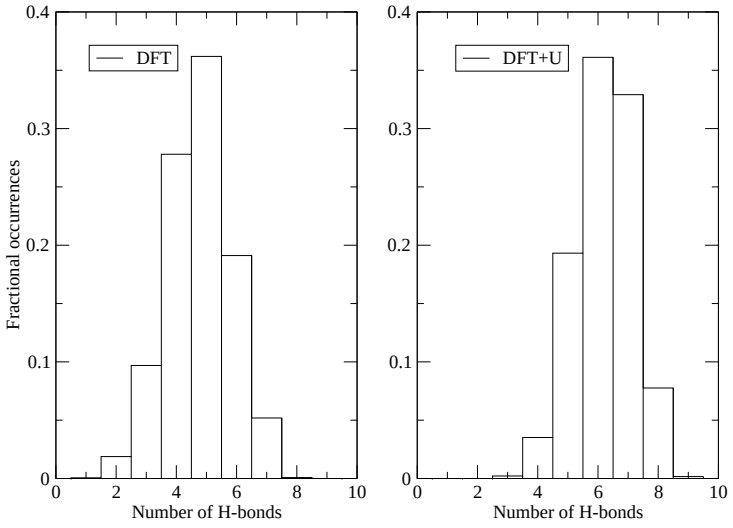


Figure 7: Total number of hydrogen bonds between the molecules of water and the S ions in the cluster during the MD runs with and without the $U$ correction.

We present the fractional occurrences in Figure 7, where it emerges that the $U$ correction applied to the Fe ions translates into an increased tendency of S ions to form hydrogen bonds. Quantatively, the average value resulting from DFT is 4.9, much lower than the 6.2 obtained by DFT+U.

## 4 Conclusions

We have presented a theoretical investigation of the $Fe_2S_2$ cluster in aqueous solution. As clearly evidenced by its poor performance on the geometry and

magnetic coupling of $Fe_2S_2$ in the gas-phase, TM clusters are a challenge for DFT. To improve the description, we have shown that it is possible to adopt the DFT+U approach, where the value of $U$ can be parameterised on the HS state geometry of $Fe_2S_2$ obtained with the high-level CCSD(T) method. It is only with this approach, that the magnetic couplings reproduce those in the literature.

When the same value of $U$ is employed for the study of $Fe_2S_2(H_2O)_8$, the DFT+U results are successful, whereas, with respect to experiments, standard DFT predicts a structure which is again too contracted, and an exchange constant which is too negative.

In both methods, the picture resulting after around 15 ps of MD in water is that of a stable $Fe_2S_2$(aq) complex, in line with experiments [2, 3]. However, compared to standard DFT, DFT+U predicts the geometry of the rhombic $Fe_2S_2$ unit to be more strecthed and not planar. Thus, the two Fe(II) can accommodate a total number of 4-5 molecules of water, rather than 3-4. Similarly, adding the $U$ term to the d-electron of $Fe_2S_2$(aq) increases the number of water molecules interacting through hydrogen bonds with the two sulfurs.

Provided that the value of $U$ is accurately fitted to reproduce relevant parameters determined by high-level quantum chemistry methods, DFT+U represents a viable approach to the study of aqueous iron-sulfur clusters, which are of interest in areas ranging from Origins of Life theories to enzyme biology and catalysis.

## Acknowledgements

We are grateful to Devis Di Tommaso for providing us with the pre-equilibrated box of water. We acknowledge the UK Natural Environment Research Council (grant NE/J010626) for funding. This work made use of the facilities of HECToR, the UK's national high-performance computing service, which is provided by UoE HPCx Ltd at the University of Edinburgh, Cray Inc and NAG Ltd, and

funded by the Office of Science and Technology through EPSRC's High End Computing Programme.

## References

[1] G. Wächtershäuser, *Syst. Appl. Microbiol.*, 1988, **10**(3), 207–210.

[2] S. M. Theberge and G. W. Luther III, *Aquat. Geochem.*, 1997, **3**(3), 191–211.

[3] G. W. Luther III and D. T. Rickard, *J. Nanopart. Res.*, 2005, **7**(4-5), 389–407.

[4] D. Rickard and G. W. Luther, *Chem. Rev.*, 2007, **107**(2), 514–562.

[5] S. Haider, D. Di Tommaso, and N. H. de Leeuw, *Phys. Chem. Chem. Phys.*, 2013, **15**(12), 4310–4319.

[6] H. Beinert, R. H. Holm, and E. Münck, *Science*, 1997, **277**(5326), 653–659.

[7] K. Koszinowski, D. Schröder, H. Schwarz, R. Liyanage, and P. Armentrout, *J. Chem. Phys.*, 2002, **117**, 10039.

[8] A. Nakajima, T. Hayase, F. Hayakawa, and K. Kaya, *Chem. Phys. Lett.*, 1997, **280**(3), 381–389.

[9] N. Zhang, T. Hayase, H. Kawamata, K. Nakao, A. Nakajima, and K. Kaya, *J. Chem. Phys.*, 1996, **104**(10), 3413–3419.

[10] L.-P. Ding, X.-Y. Kuang, P. Shao, and M.-M. Zhong, *J. Mol. Model.*, 2012, pp. 1–10.

[11] Y.-N. Li, S. Wang, T. Wang, R. Gao, C.-Y. Geng, Y.-W. Li, J. Wang, and H. Jiao, *ChemPhysChem*, 2013, **14**(6), 1182–1189.

[12] S. Tazibt, S. Bouarab, A. Ziane, J. Parlebas, and C. Demangeat, *J. Phys. B: At., Mol. Opt. Phys.*, 2010, **43**(16), 165101.

[13] M. D. Esrafili, S. Rezaei, and E. Eftekhari, *Comput. Theor. Chem.*, 2012.

[14] O. Hübner and J. Sauer, *J. Chem. Phys.*, 2002, **116**, 617.

[15] O. Hübner and J. Sauer, *Phys. Chem. Chem. Phys.*, 2002, **4**(21), 5234–5243.

[16] P. Venkateswara Rao and R. Holm, *Chem. Rev.*, 2004, **104**(2), 527–560.

[17] M. F. Verhagen, T. A. Link, and W. R. Hagen, *FEBS lett.*, 1995, **361**(1), 75–78.

[18] E. J. Leggate, E. Bill, T. Essigke, G. M. Ullmann, and J. Hirst, *Proc. Natl. Acad. Sci. U. S. A.*, 2004, **101**(30), 10913–10918.

[19] S. J. Yoo, J. Meyer, and E. Münck, *J. Am. Chem. Soc.*, 1999, **121**(44), 10450–10451.

[20] W. Yao, P. M. Gurubasavaraj, and P. L. Holland, Springer Berlin Heidelberg, 2012; pp. 1–37; Structure and Bonding.

[21] B. Himmetoglu, A. Floris, S. Gironcoli, and M. Cococcioni, *Int. J. Quantum Chem.*, 2014, **114**(1), 14–49.

[22] N. N. Nair, E. Schreiner, R. Pollet, V. Staemmler, and D. Marx, *J. Chem. Theory Comput.*, 2008, **4**(8), 1174–1188.

[23] D. Bovi and L. Guidoni, *J. Chem. Phys.*, 2012, **137**, 114107.

[24] A. Ghosh and P. R. Taylor, *Curr. Opin. Chem. Biol.*, 2003, **7**(1), 113–124.

[25] K. Leung and C. J. Medforth, *J. Chem. Phys.*, 2007, **126**, 024501.

[26] D. Jiao, K. Leung, S. B. Rempe, and T. M. Nenoff, *J. Chem. Theory Comput.*, 2011, **7**(2), 485–495.

[27] S. Dudarev, G. Botton, S. Savrasov, C. Humphreys, and A. Sutton, *Phys. Rev. B*, 1998, **57**(3), 1505–1509.

[28] M. Cococcioni and S. de Gironcoli, *Phys. Rev. B*, 2005, **71**(3), 035105.

[29] A. J. Devey, R. Grau-Crespo, and N. H. de Leeuw, *Phys. Rev. B*, 2009, **79**, 195126.

[30] A. Roldan, D. Santos-Carballal, and N. de Leeuw, *J. Chem. Phys.*, 2013, **138**, 204712.

[31] A. Devey and N. de Leeuw, *Phys. Rev. B*, 2010, **82**(23), 235112.

[32] A. Krishnamoorthy, F. W. Herbert, S. Yip, K. J. Van Vliet, and B. Yildiz, *J. Phys.: Condens. Matter*, 2013, **25**(4), 045004.

[33] P. Lazić, R. Armiento, F. Herbert, R. Chakraborty, R. Sun, M. Chan, K. Hartman, T. Buonassisi, B. Yildiz, and G. Ceder, *J. Phys.: Condens. Matter*, 2013, **25**(46), 465801.

[34] G. Rollmann, H. C. Herper, and P. Entel, *J. Phys. Chem. A*, 2006, **110**(37), 10799–10804.

[35] H. J. Kulik, M. Cococcioni, D. A. Scherlis, and N. Marzari, *Phys. Rev. Lett.*, 2006, **97**(10), 103001.

[36] N. N. Nair, J. Ribas-Arino, V. Staemmler, and D. Marx, *J. Chem. Theory Comput.*, 2010, **6**(2), 569–575.

[37] A. Albers, S. Demeshko, K. Propper, S. Dechert, E. Bill, and F. Meyer, *J. Am. Chem. Soc.*, 2013, **135**(5), 1704–1707.

[38] F. Neese, *Coord. Chem. Rev.*, 2009, **253**(5), 526–563.

[39] A. Dey, *Inorg. Chem.*, 2011, **50**(2), 397–399.

[40] M. Frisch, G. Trucks, H. B. Schlegel, G. Scuseria, M. Robb, J. Cheeseman, G. Scalmani, V. Barone, B. Mennucci, G. Petersson, et al., *Gaussian Inc., Wallingford*, 2009.

[41] G. Kresse and J. Hafner, *Phys. Rev. B*, 1993, **47**(1), 558–561.

[42] G. Kresse and J. Furthmuller, *Comput. Mater. Sci.*, 1996, **6**(1), 15–50.

[43] T. H. Dunning Jr, *J. Chem. Phys.*, 1989, **90**, 1007.

[44] J. P. Perdew, K. Burke, and M. Ernzerhof, *Phys. Rev. Lett.*, 1996, **77**(18), 3865.

[45] Y. Zhao and D. G. Truhlar, *J. Chem. Phys.*, 2006, **125**(19), 194101.

[46] P. E. Blöchl, *Phys. Rev. B*, 1994, **50**(24), 17953.

[47] S. Nosé, *J. Chem. Phys.*, 1984, **81**, 511.

[48] P.-L. Sit and N. Marzari, *J. Chem. Phys.*, 2005, **122**, 204510.

[49] P. J. Hay and W. R. Wadt, *J. Chem. Phys.*, 1985, **82**(1), 270–283.

[50] M. Dolg, U. Wedig, H. Stoll, and H. Preuss, *J. Chem. Phys.*, 1987, **86**(2), 866–872.

[51] M. Bühl and H. Kabrede, *J. Chem. Theory Comput.*, 2006, **2**(5), 1282–1290.

[52] D. Rickard and J. W. Morse, *Mar. Chem.*, 2005, **97**(3), 141–197.

[53] A. Dey, F. E. Jenney, M. W. Adams, E. Babini, Y. Takahashi, K. Fukuyama, K. O. Hodgson, B. Hedman, and E. I. Solomon, *Science*, 2007, **318**(5855), 1464–1468.

[54] A. Dey, T.-a. Okamura, N. Ueyama, B. Hedman, K. O. Hodgson, and E. I. Solomon, *J. Am. Chem. Soc.*, 2005, **127**(34), 12046–12053.

[55] K. Rose, S. E. Shadle, T. Glaser, S. de Vries, A. Cherepanov, G. W. Canters, B. Hedman, K. O. Hodgson, and E. I. Solomon, *J. Am. Chem. Soc.*, 1999, **121**(11), 2353–2363.

[56] T. Glaser, B. Hedman, K. O. Hodgson, and E. I. Solomon, *Acc. Chem. Res.*, 2000, **33**(12), 859–868.

[57] T. Glaser, I. Bertini, J. J. Moura, B. Hedman, K. O. Hodgson, and E. I. Solomon, *J. Am. Chem. Soc.*, 2001, **123**(20), 4859–4860.

[58] A. Dey, C. L. Roche, M. A. Walters, K. O. Hodgson, B. Hedman, and E. I. Solomon, *Inorg. Chem.*, 2005, **44**(23), 8349–8354.

[59] T.-a. Okamura, S. Takamizawa, N. Ueyama, and A. Nakamura, *Inorg. Chem.*, 1998, **37**(1), 18–28.

[60] T. Todorova, A. P. Seitsonen, J. Hutter, I.-F. W. Kuo, and C. J. Mundy, *J. Phys. Chem. B*, 2006, **110**(8), 3685–3691.

[61] I.-C. Lin, A. P. Seitsonen, M. D. Coutinho-Neto, I. Tavernelli, and U. Rothlisberger, *J. Phys. Chem. B*, 2009, **113**(4), 1127–1131.

[62] C. Adamo and V. Barone, *J. Chem. Phys.*, 1999, **110**(13), 6158–6170.

[63] S. Grimme, *J. Comput. Chem.*, 2006, **27**(15), 1787–1799.